Solid State Phenomena
ISSN: 1662-9779, Vol. 359, pp 13-20
doi:10.4028/p-FcSm9i

Submitted: 2023-09-04
Revised: 2023-09-06
Accepted: 2024-05-21
Online: 2024-08-22

Evolution of the Substitutional Fraction on Post-Implantation Annealing in Al/4H-SiC Systems

Virginia Boldrini[1,a], Antonella Parisini[2,b] and Marco Pieruccini[1,c*]

[1]CNR-Institute for Microelectronics and Microsystems, v. Piero Gobetti 101, 40129 Bologna, Italy

[2]Dipartimento di Scienze Matematiche, Fisiche e Informatiche (SMFI), Università di Parma, Parco Area delle Scienze 7/A,43124 Parma, Italy

[a]boldrini@bo.imm.cnr.it, [b]antonella.parisini@unipr.it, [c]pieruccini@bo.imm.cnr.it

Keywords: Statistical Mechanics, Cooperativity, Implantation, Annealing, 4H-SiC.

Abstract. The problem of crystal damage recovery and of impurity substitution in implanted semiconductors is considered from a statistical mechanical viewpoint. This is done by resorting to a thermodynamic pseudo-potential originally developed for cooperative structural rearrangements in disordered systems close to their glass transition. The dependence of the substitutional fraction φ on the post-implantation annealing temperature T_{ann} in Al/4H-SiC systems is discussed in the light of these ideas. After completion of the annealing process, an Arrhenius plot of $\varphi(T_{ann})$ shows a slope in the order of 1 eV or less, depending on the amount of lattice damage initially produced by the implantation. Slopes $\sim$4 eV are found after incomplete annealing, indicating that substitution occurs mainly in damaged crystal cells. These concepts are suggested to be used for optimization of the doping procedure by ion implantation.

Introduction

When ion implantation is used for tailoring the electrical properties of semiconductors, one necessarily copes with the problems of crystal damage recovery and electrical activation, which are relevant during both implantation and post-implantation annealing. Below, we shall focus mainly on the latter process.

From the thermodynamic point of view, an *un*-annealed implanted system resides in a metastable state: a relative minimum of the free energy that needs sufficient heating to be abandoned. Once the conditions for escaping this free energy well are reached, the system will rearrange trying to approach crystal regularity, where the free energy would be lowest (at temperatures T where the crystal phase is stable). Implanted impurities may become substitutional during this relaxation process.

As a working hypothesis, we consider the wandering of this system through successive metastable states in analogy with the behavior of non-crystallizable *liquids* (e.g. some polymeric melts) close to their glass transition. Indeed, these liquids explore, in a restless wandering, a succession of different structural states, each one with its own residence time related to the depth of its energy well. The transition from one well to the next, i.e. a structural transition, is governed by the contact with the heat bath through the vibrational degrees of freedom.

We shall see that this analogy allows to rationalize results of the literature concerning how the annealing temperature T_{ann} and the annealing time τ_{ann} influence the final substitutional fraction φ.

This topic has been the focus of a recently published paper [1]; here, we shall deal with issues that could not be treated in that contribution, so the present one can be considered complementary to it.

The thermodynamic pseudo-potential relevant to the description of the structural evolution in quasi-equilibrium liquids is first introduced. Then, a simple view of the elementary substitution processes is proposed, in the light of which some literature data are discussed. This scheme will also indicate the main directions whereby the approach can be extended to cover the implantation process itself.

Theory

Thermodynamic pseudo-potential. On general grounds we consider a disordered system (in contact with a heat bath) as made of two interpenetrated subsystems: one collecting the conformational (or configurational, interchangeably), long range and slow, degrees of freedom (d.o.f.), the other consisting of the fast vibrational ones, including those of collective/oscillatory nature. Though non-zero, their *direct* mutual interaction is weak, that is, the partition function of the whole system would be approximately $Z_{tot} \cong Z_{conf} Z_{vib}$ (cf. ref. [2]), with obvious notation. Nevertheless, a mutual influence does exist through a particular subset of collective/oscillatory d.o.f. [see comment after Eq. (5) below]; the way it is accounted for can be understood by referring to Fig. 1, where a hypothetic conformational evolution is represented.

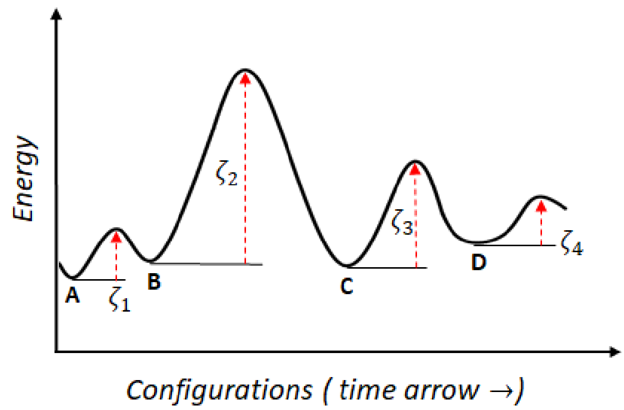

Fig.1 Schematic of the *random* evolution in the energy of a rearranging system; {A, B, C, D, …} and {ζ_1, ζ_2… ζ_i ...} are the time-ordered sequences of quasi-stable conformations and, respectively, energy barriers that need be crossed to escape them, allowing for structural transitions. For convenience the energy is *per unit* (atom, monomer,…) forming the system.

We consider the persistence of the system in a given structural state (A, B, C, … in Fig. 1) as the effect of transient constraints; the deeper the i-th energy well (i.e. the larger ζ_i in Fig. 1) , the stronger the constraint, the longer the residence time in the well. There are two main mechanisms defining the mutual interference between conformations and collective oscillations: i) the actual energy barrier ζ_i is determined by the conformation and ii) localized collective oscillatory modes (localized phonons) *may* stimulate structural transitions (say from B to C) if each unit involved in the mode has gained an energy $\epsilon \geq \zeta_i$.

The partition function Z_{conf} is now constructed starting from the entropy. Assuming that there is no degeneracy, we classify different structural states by their well depth (or barrier height) ζ; from their occurrence probability p_ζ, we define the *specific* entropy

$$S_{conf} = -k_B \sum_\zeta p_\zeta \ln p_\zeta \, , \tag{1}$$

where k_B is the Boltzmann constant.

The energy per unit that allows to probe next conformation from a ζ-labeled state, must reside initially in the fast collective d.o.f. and is given by

$$\langle E \rangle_\zeta = W_\zeta^{-1} \sum_{\epsilon \geq \zeta} \epsilon \, w_\epsilon \, , \tag{2}$$

where $W_\zeta \equiv \sum_{\epsilon \geq \zeta} w_\epsilon$ is the overall probability that this unit gains, through the excitation of local collective modes, an energy $\epsilon > \zeta$ above the ground state (in the spirit of our approximate Z_{tot} factorization, both w_ϵ and W_ζ are almost independent of the actual conformation, i.e. A, B, C, … in Fig. 1). On turn, the time-average of this energy is $U_\zeta = W_\zeta \langle E \rangle_\zeta$.

One can easily relate W_ζ to the lack of entropy accompanying the quenching of configurational modes (i.e. the presence of constraints to the long range d.o.f.) through the following reasoning. As shown in Fig. 2, at constant E_{tot} the total equilibrium entropy S_{eq} of the system *plus* the heat bath changes by $\Delta S < 0$ when long range modes quench; the representative point of the composite system thus moves from *a* to *b* in the figure. The same state can be reached through an isentropic path from point *c* by performing reversible work from an external source on the fast collective d.o.f. (the conformational ones being quenched), that is, increasing the free energy of the system by $N\overline{\Delta\mu_\zeta}$, where the bar stands for p_ζ-average, N is the number of units in the system and $\Delta\mu_\zeta = -k_B T \ln W_\zeta$ [3]. In terms of the specific configurational entropy $s_c \equiv -\Delta S/N$, one finds:

$$Ts_c = \overline{\Delta\mu_\zeta} \,. \tag{3}$$

In our scheme, the sequence $c \to b \to a$ can also be viewed as the path through which thermodynamic equilibrium at E_{tot} can be recovered: Ts_c plays the role of rearrangement threshold for $\overline{\Delta\mu_\zeta}$ [4].

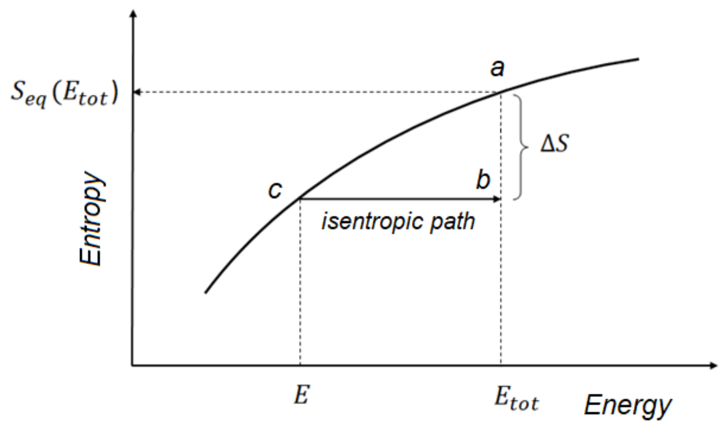

Fig. 2. Entropy of the composite system (i.e. including the heat bath) as a function of its energy, and effect on S_{eq} of a source of non-equilibrium (temperature differences between system and heat bath, transient quenching of long range modes, etc.).

The configurational specific free energy is found, together with the appropriate p_ζ distribution, by extremizing the difference $\overline{U_\zeta} - TS_{conf}$ under the condition that $\overline{\Delta\mu_\zeta} = const$. This yields

$$f = -k_B T \ln Z_{conf} + \mu_0 \,, \qquad Z_{conf} \equiv \textstyle\sum_\zeta {W_\zeta}^\lambda \, e^{-W_\zeta \langle E\rangle_\zeta / k_B T} \tag{4}$$

where λ is the Lagrange multiplier associated to the constraint on $\overline{\Delta\mu_\zeta}$, and a bias contribution μ_0 usually encompassed in Ts_c (e.g. in case hydrogen bindings need be weakened before rearrangements are allowed) has been included. Analyses of relaxation experiments (cf. e.g. [4-6]) indicate that $\lambda \approx n$, where n is the best fitting *mean* number of units participating the collective oscillatory motion *precursory* to structural rearrangements at a given T. For n normal harmonic oscillators one has

$$W_\zeta \equiv W_{\zeta,n} = Z_{\zeta,n}/Z_n \,, \qquad Z_{\zeta,n} = \textstyle\sum_{\epsilon\geq\zeta} \epsilon^{n-1} e^{-\epsilon/k_B T} \,, \qquad Z_n \equiv Z_{\zeta,n}\big|_{\zeta=0} \,. \tag{5}$$

Modes with different n can be viewed as independent *states/particles* of different nature; thus, $Z_{vib} \propto \prod_n Z_n$, its influence on Z_{conf} appearing as mainly due to the component $Z_\lambda = Z_n|_{n=\lambda}$. This highlights the *mean-field* character of the theory, calling for an improvement which is now underway.

The λ-units' joint probability ${W_\zeta}^\lambda$ in Eq. (4) can be expressed as ${W_\zeta}^\lambda = e^{-\lambda\Delta\mu_\zeta/k_B T}$, that is, $\lambda\Delta\mu_\zeta$ is the missing energy completing the Boltzmann factors of Z_{conf} in Eq. (4); in other words $\lambda\,\overline{\Delta\mu_\zeta} \approx \overline{(1 - W_\zeta)\,\langle E\rangle_\zeta}$. Hence, one may readily see that if a dominant, maximum energy barrier ζ_{max} needs be crossed for rearrangement, then it must be related to the *cooperativity* λ by [remind Eq. (3)]

$$\lambda \sim \zeta_{max}/(Ts_c - \mu_0) \,. \tag{6}$$

This relation also holds in the initial stages of the cooperative rearrangement in an implanted system.

Substitution and damage recovery. Non-extended defects are localized metastable conformational states; localization is in fact also an aspect of the confinement due to the embedding crystal phase. If an Al-impurity is present in one such region, it may substitute a Si atom as a consequence of cooperative rearrangements. The disordered region first reaches by cooperative motions a *transient state*, with only one Si-lattice bond still remaining (we call this state a *trial*); then, further motions set in where this last bond may break, allowing for substitution. There is a limit in the number of possible trials, because the system is evolving, trial by trial, towards a structural arrest (either in an ordered state or, once again, in another local and deeper metastable state).

As illustrated previously, the defective region is in thermodynamic equilibrium during cooperative rearrangements and, in particular, during a trial; thus, if Ω_i and Ω_f are the degeneracies of the initial state (just one Si-lattice bond left) and, respectively, of the state where the last bond is broken, the partition function of the trial state is $\mathcal{Z}_c = \Omega_i + \Omega_f e^{-\Delta E_s/k_B T}$. From this, it can be shown that the substitutional fraction φ after *sufficient annealing time*, that is, the fraction φ_∞ in the asymptotic state, is approximately [1]:

$$\varphi_\infty \cong N_t e^{-\Delta E_s/k_B T} \Omega_f/\Omega_i \quad , \tag{7}$$

where ΔE_s is the energy of last Si-lattice bond, which for 4H-SiC is in the order of 1 eV or less, depending on the initial lattice damage [1], and N_t is the average number of trials each Al-impurity undergoes before structural arrest. One can estimate $\Omega_f \sim \lambda_t \Omega_i$, where λ_t is the cooperativity of the trial (which is indeed related to the size of the cooperative region), that is, we assume that the Si atom just detached from the lattice, wanders about occupying a number of positions in the order of λ_t; this is to say that $s_w \equiv s_c - \mu_0/T \approx k_B \ln \lambda_t$ is the *wandering* (or topological, interchangeably) entropy of the unbinded Si. Since a trial requires an energy fluctuation $\Delta E_w \approx 3$ eV (see below), from the wandering entropy of Si and from Eq. (6) one finds a cooperativity $\lambda_t \approx 10$ for $1500 \leq T \leq 1900$ °C (this is of course a gross estimate since a cooperative rearrangement proceeds by facilitation [1,5], triggered by a number $z \leq \lambda$ of atoms which increases as an effect of confinement [6], i.e. by the embedding crystal phase; it is indeed the fluctuation energy $\approx z\,\overline{\Delta\mu_\zeta}$ that appears as ΔE_w).

In order to relate the effective number N_t of trials to their formation rate, $\propto e^{-\Delta E_w/k_B T}$, one should describe the time evolution of the damage recovery. This will be next target in the application of cooperativity concepts to the present problems. We can just say that if the trial frequency is $\nu \sim \nu_0 e^{-\Delta E_w/k_B T}$, with ν_0 an attempt rate, the approach to a structural arrest could be described by an effective ΔE_w which increases in time. Hence one may write

$$N_t \sim \int_0^{\tau_{ann}} \nu_0 e^{-\Delta E_w(\tau)/k_B T}\, d\tau \quad , \tag{8}$$

where τ_{ann} is the post-implantation annealing time. As a rough model, one may take a constant $\Delta E_w(\tau)$ in the interval $0 \leq \tau \leq \nu^{-1} < \tau_{ann}$, which suddenly increases afterwards; this provides us with a number of trials that is almost independent of T. We note that a structural arrest may be reached not only when the crystalline order is locally recovered, but also when confinement by the embedding crystal imposes a severe limit to λ (or to the size of the rearranging region anyway): an available volume smaller than that needed for cooperative rearrangement quenches the rearrangement itself. This is in fact what happens when T is lowered, forcing the damaged region in a metastable state. On the contrary, upon rising T, λ decreases and the region becomes free to rearrange. This is clearly pointed out by Eq. (6), which in terms of s_w reads $\lambda \sim \Delta E_w/T s_w$.

Analysis of Literature Data

We consider first the dependence of φ_∞ on the annealing temperature T_{ann} reported in [7], All samples were implanted up to an ion concentration of 2.25×10^{19} cm^{-3} within a layer of 600 nm thickness; 30-min post-implantation thermal treatments were then imposed. The data are represented as triangles in Fig. 3 and refer to two different implantation temperatures: room temperature (RT) and $T_{impl} = 500$ °C (full and open symbols respectively).

In both cases the annealing time resulted long enough to reach the asymptotic state, however RT implantation leaves the system with a larger number of displaced Si atoms as compared to the higher temperature implantation [7], that is, beam-lattice collisions alone cannot be as effective as when $T_{impl} = 500$ °C in stimulating damage recovery or partial Al-substitution *during* implantation. In other words, at the beginning of the annealing treatments the RT-implanted systems are more disordered; consistently, the $\ln \varphi_\infty$ vs. $1/k_B T_{ann}$ slope of the RT-implanted samples (0.58 eV) is lower than for the others (0.77 eV).

On the other hand, both $\ln \varphi_\infty$ and $N_t \Omega_f / \Omega_i$ drop on decreasing T_{impl} (the latter from $\sim$80 down to $\sim$20); that is, in a more damaged lattice substitution comes to completion faster and less efficiently. The reason is that N_t is limited by the rate at which the distorted regions approach a structural arrest; for a more damaged lattice this rate is higher, which has to be related to lower cooperativities.

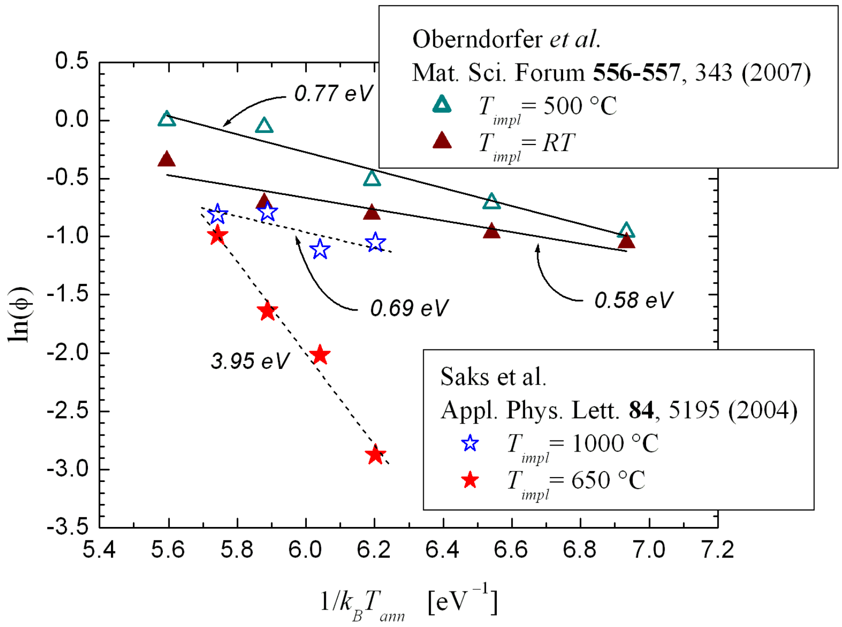

Fig. 3. Logarithm of the substitutional fraction φ as a function of the inverse thermal energy $k_B T_{ann}$ at the annealing temperature. Ref. [7] data as well as those of ref.[8] show effects of a change in T_{impl} (unfortunately further information about the implantation schedules is lacking).

In order to discuss incomplete annealing, instead, we consider the data of ref. [8], which refer to samples implanted with final Al density of 2×10^{20} cm^{-3} within a layer of 200 nm thickness. The Hall mobility and carrier density T-dependencies in ref. [8] have been re-analyzed with the method of ref. [9] in order to work out $\varphi(T_{ann})$; the results are plotted in Fig. 3 as stars. Open symbols refer to implantations carried out at $T_{impl} = 1000$ °C, solid ones at $T_{impl} = 650$ °C; in both cases, the samples underwent 5-min post-implantation annealing.

Despite the lack of further information, we can say that for the 650 °C implanted samples the annealing is incomplete: 5 minutes are not enough to reach a structural arrest, and the fluctuation dynamics underlying the attainment of the transient states (the trials) still shows up through the slope of $\varphi(T_{ann})$ in Fig. 3 ($\sim$4 eV); indeed, in the early stages of the annealing process $\varphi(t;T) \sim \nu_0 t e^{-(\Delta E_w + \Delta E_s)/k_B T}$ [1]. For this reason no estimate is worth for N_t in this case.

What is happening *during* the 1000 °C implantation is difficult to say at present. The final slope is 0.69 eV, but it is hardly reasonable to think that 5 min annealing now became sufficient to reach a structural arrest, posing a limit to N_t in this way. Rather, it is more likely that structural arrest was already closely approached during the implantation process. In this situation, post-implantation annealing only drives to the end uncompleted substitution events, or acts in fact as a re-annealing at $T_{ann} > T_{impl}$. The latter can be effective because there is always a Si atom close to an interstitial Al (which itself creates a slight local deformation of the lattice), and an increase of T simply enhances the substitution probability $\sim e^{-\Delta E_s / k_B T}$. Thus, the trend shown by the open stars in Fig. 3 would not result from the mechanism described by Eq. (7), but would be just a re-modulation of a substitutional fraction established already, or about to be established, during implantation. Notwithstanding this picture, yet we provide a worked out *apparent* effective trial number of $N_t\Omega_f/\Omega_i \cong 25$. Comparing it to the value of ~ 20 found for the RT implanted systems of ref. [7], means envisaging a hypothetic connection between post-implantation annealing from a highly disordered state (T_{impl} = RT in ref. [7]), and a relatively efficient ($T_{impl} = 1000$ °C in ref. [8]) recovery contrasting significant damage production while implanting [10]. Of course, the number of trials is not determined only by thermal excitations during implantation, since also the energy delivered by colliding ions plays its role in this process; for this reason, Eq. (8) is not valid in this case.

Optimization of Implant Conditions

The present study poses the basis for an optimization methodology of ion implantation and subsequent annealing processes, providing an interpretative key of the electrical data obtained by properly varying T_{impl}, and the temperature T_{ann} and time duration τ_{ann} of the subsequent annealing treatments, given an implantation density N_{impl}. In ref. [1] it was shown that both resistivity and fraction φ of electrically activated implanted ions show an Arrhenian dependence on T_{ann}, the latter having been justified in this work in terms of cooperativity, the former being a statistically significant empirical result. The mutual consistency in the behaviors of these two quantities, and in particular the similarities of the Arrhenian slopes, relies in that an approximate saturation of substitution events is expected to take place in times much shorter than the subsequent improvement of crystalline quality underlying the continuous increase of both drift carrier density and mobility observed at ever increasing τ_{ann} [11]. In fact, a reduction of compensating defects can lead to an increase of the net doping level without implying an increase of the acceptor density, also enhancing mobility thanks to the reduction of the ionized scattering centers. This indicates that there are electrically active structural defects acting as compensating centers, and that the time evolution of their recovery extends after the Al-substitution completion, but with minor effects. Due to the slow settling of lattice defects, resistivity and fraction φ of electrically activated impurities can roughly have the same dependence on T_{ann}, being dominated by the Al-substitution process.

Certainly the study of the Arrhenius plot of the RT resistivity vs. T_{ann}, for fixed and controlled values of τ_{ann}, T_{impl} and implant dose, is a simple way to establish when the asymptotic state is reached, and the minimum τ_{ann} needed for this. An Arrhenian slope of the low-T resistivity (or φ) vs. T_{ann} significantly higher than unity indicates structural arrest before reaching the asymptotic state; on the contrary, values around unity suggest that φ_∞ was approached, although the lower the value below unity, the higher the *pre*-annealing disorder is expected to be.

In order to identify the optimal conditions (implant + annealing) for maximal doping efficiency, reliable information on the *pre*-annealing crystalline quality can be obtained by an accurate evaluation of ΔE_s and N_t; to this aim, an estimation of φ should be searched which, given N_{impl}, requires the determination of the dopant density N_A (acceptors in this work) by fitting Hall data.

Despite the lack of further information, a complete analysis of the electrical data permits to obtain *i*) the density of activated dopants and compensating defects for each sample, the latter being expected to provide information on the *post*-annealing disorder, and *ii*) ΔE_s and $N_t\Omega_f/\Omega_i$ from the φ_∞ vs. T_{ann} dependence at fixed N_{impl}, T_{impl}, τ_{ann}, assuming $\varphi_\infty = N_A/N_{impl}$.

In ref. [9], a method for the simultaneous analysis (i.e. with shared fitting parameters) of Hall density (n_H) *and* mobility data is proposed, which is more reliable than the simple fitting of only $n_H(T)$ often carried out in the literature. The latter was used in ref. [7] to derive the data of Fig. 3 (triangles), which nevertheless have been considered here just to discuss a trend; a complete electrical characterization was in fact available *only* for the $T_{impl} = 500$ °C samples. Using the approach of ref. [9] on these samples, the values $\ln \varphi_\infty|_{T_{ann}=1800\,°\mathrm{C}} \cong -0.9$, $\Delta E_s = 0.98$ eV and $N_t\Omega_f/\Omega_i \cong 100$ are found [1], which stresses the critical role of the chosen method of analysis for inferring quantitatively reliable conclusions (note that $\ln \varphi_\infty|_{T_{ann}=1800\ °C} \cong 0$, as indicated by the open triangle data in Fig. 3).

A comparison between the ΔE_s values obtained for different data sets gives relative information on lattice damage *at the end* of implantation and *before* annealing, which is very useful when all implantation parameters (including e.g. the dose rate) are known and varied in a controlled way. On the other hand, mobility is sensitive to disorder *after* annealing. As an example, Fig.4 compares the drift transport data of 1600 °C annealed samples of refs. [7] and [8] which are subsequently fitted by the method of ref. [9]. Notice that drift data reported in the figure, i.e. corrected for the Hall factor [9], are self-consistently calculated in the fitting procedure. Activated acceptor densities of 5.1×10^{18} cm^{-3} for ref. [7] and 6.28×10^{19} cm^{-3} for ref. [8] samples were found, corresponding to activation efficiencies of about 0.23 and 0.35 respectively; compensation ratios (i.e. the fractions of compensating defects within the activated acceptors) about 0.2-0.3 are obtained for both. The comparison of the results points out that the higher implant density (and N_A doping level) of the ref. [8] sample with respect to the ref. [7] one, does not lead to a significantly higher carrier density at ordinary temperatures, rather it is detrimental, because it decreases the mobility, indicating a higher level of disorder *after* the annealing treatment. This would be consistent with the indications from ΔE_s and $N_t\Omega_f/\Omega_i$ of high disorder already *before* the annealing, although it is not known how these quantities would evolve in case of a prolonged annealing on ref. [8] samples.

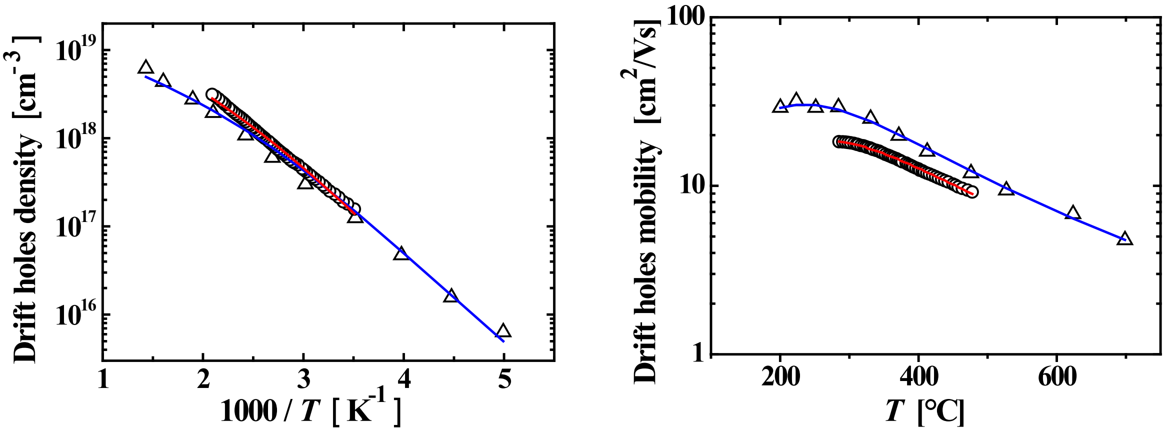

Fig.4 Drift hole densities (left) and mobilities (right) as functions of the sample temperature for two samples subjected to annealing at T_{ann}=1600 °C, for which the asymptotic state was reached: triangles are from ref. [7] with $T_{impl} = 500$ °C and $\tau_{ann} = 30$ min; circles are from ref. [8] with $T_{impl} = 1000$ °C and $\tau_{ann} = 5$ min. Solid lines are obtained by simultaneous fittings of both hole densities and mobilities, following the transport model of ref. [9].

Summary

The theme of cooperativity seems to provide a help in discussing observations concerning the efficiency of impurity ion substitution after thermal treatments in implanted semiconductors. In fact, the arguments are general, and are expected to be worth also in systems other than Al-implanted 4H-SiC.

The experiments discussed above point out that for long enough annealing times ($\tau_{ann} = 30$ min for $1500 \leq T_{ann} \leq 1900$ °C) the slope in an Arrhenius representation of the φ_∞ (or φ) vs. T dependence is not larger than $\Delta E_{s,max} \approx 1$ eV (this value may be different for other semiconductors or impurities) [1]; larger slopes are indicative of incomplete annealing. In the latter case we worked out an activation energy of $\Delta E_w \cong 3$ eV for the attainment of a trial state. Since this energy is significantly lower than the formation of a Si vacancy in a regular lattice (i.e. about 6 eV, at least for 3C-SiC, after the simulations in ref. [12]), we conclude that substitutions mainly occur in damaged sites. On the other hand, less damaged lattices recover in longer times, which would in principle allow for larger N_t and φ_∞. For this reason, it is important to find the conditions to tailor lattice damage in an optimal way. In this respect, the correct choice of implantation protocols plays a fundamental role, as has been commented on above.

Cooperativity concepts are expected to provide a useful tool to work out at least a coarse-grained model for predicting optimal implantation condition, in particular as a route for efficient post-implantation thermal treatments.

References

[1] V. Boldrini, A. Parisini and M. Pieruccini, Analysis of the electrical activation in thermally annealed implanted Al/4H-SiC systems: A novel approach based on cooperativity, Mat. Sci. Semicond. Proc., 148 (2022) 106825

[2] M. Pieruccini and T.A. Ezquerra, Segmental relaxation in semicrystalline polymers: A mean-field model for the distribution of relaxation times in confined regimes, Eur. Phys. J. E, 29 (2009) 163-171

[3] L.D. Landau and E.M. Lifšits, Statistical Physics, part I, Pergamon Press, New York, 1980

[4] M. Pieruccini and A. Alessandrini, Method for estimating the cooperativity length in polymers, Phys. Rev. E, 91 (2015) 052603

[5] E. Tombari and M. Pieruccini, Cooperativity at the glass transition: A perspective from facilitation on the analysis of relaxation in modulated calorimetry, Phys. Rev. E, 94 (2016) 052504

[6] N. Sebastián, Ch. Contal, A. Sánchez-Ferrer and M. Pieruccini, Interplay between structure and relaxation in polyurea networks: the point of view from a novel method of cooperativity analysis of dielectric response, Soft Matter, 14 (2018) 7839-7849

[7] M. Oberndorfer, M. Krieger, F. Schmid, H.B. Weber, G. Pensl and A. Schöner, Electrical and structural properties of Al-implanted and annealed 4H-SiC, Mat. Sci. Forum 556-557 (2007) 343-346

[8] N.S. Saks, A.V.Suvorov and D.C. Capell, High temperature high-dose implantation of aluminium in 4H-SiC, Appl. Phys. Lett., 84 (2004) 5195-5197

[9] A. Parisini and R. Nipoti, Analysis of the hole transport through valence band states in heavy Al doped 4H-SiC by ion implantation, J. Appl. Phys., 114 (2013) 243703

[10] A.Yu. Kuznetsov, J. Wong-Leung, A Hallén, C Jagadish and B.G. Svensson, Dynamic annealing in ion implanted SiC: Flux versus temperature dependence, J. Appl. Phys. 94(11) (2003) 7112-7115

[11] R. Nipoti, A. Parisini, Al^+ Ion Implanted 4H-SiC: electrical activation versus annealing time, ECS Transactions, 92 7 (2019) 91-98

[12] M. Bockstedte, A. Mattausch and O. Pankratov, *Ab initio* study of the migration of intrinsic defects in 3C-SiC, Phys. Rev. B, 68 (2003) 205201